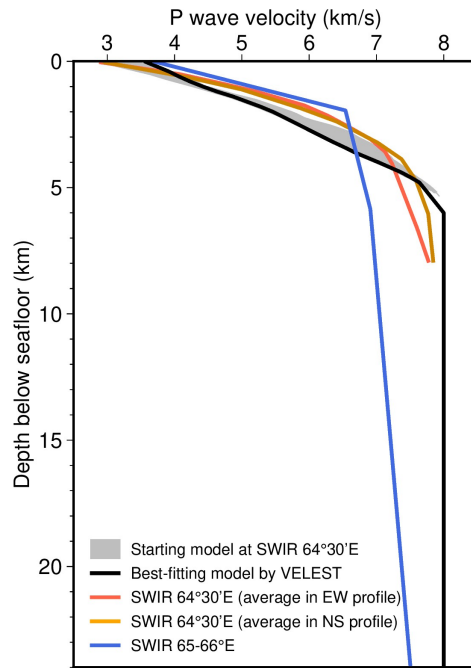


414

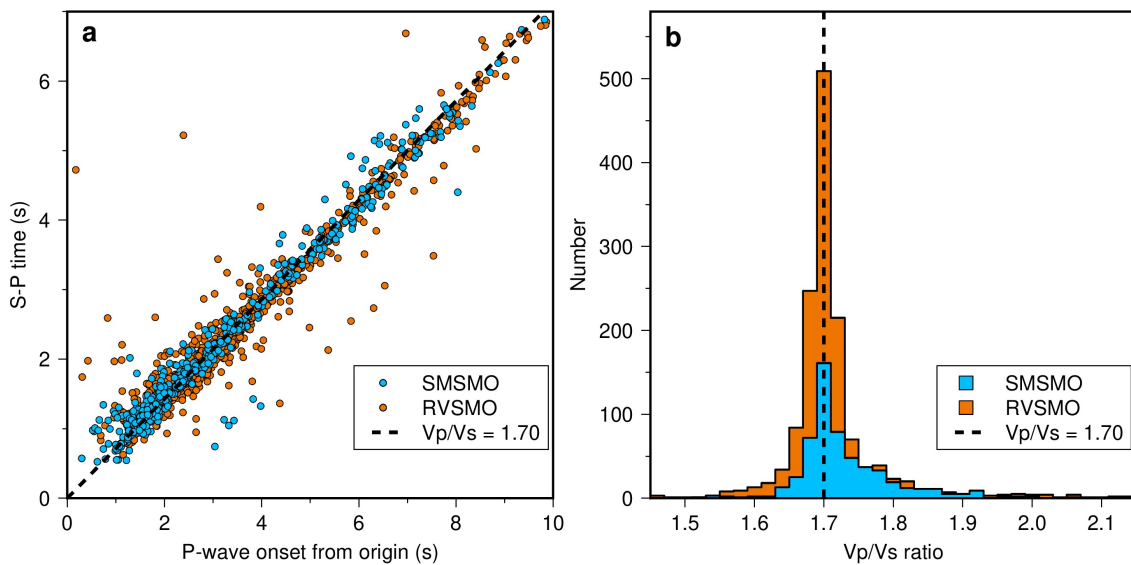
415 **Supplementary Fig. 1 | Typical event waveforms.** The event occurred at
 416 64.394°E/27.883°S 11.7 km below seafloor with a local magnitude of 2.3, at 10:56, 23 Dec
 417 2016 in RVSMO catalog. The inset shows the P-wave arrival absolute time versus arrival
 418 time differences of P- and S-waves (S-P time), yielding the origin time (T_0) of 10:56:32.3
 419 and a V_p/V_s ratio of 1.7.

420



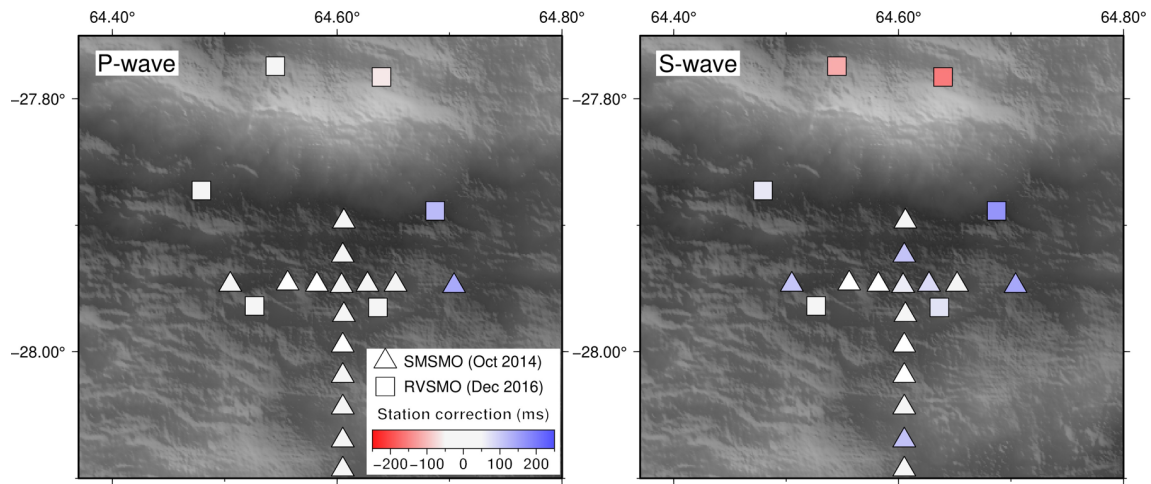
421

422 **Supplementary Fig. 2 | 1-D P wave velocity model.** Starting model (gray area) at the SWIR
 423 64°30'E is extracted from a seismic refraction experiment²³. The best-fitting model (black
 424 line) is iteratively searched by the VELEST program³⁸. Red and orange lines are average
 425 velocity models in EW and NS profiles at the SWIR 64°30'E³⁹. Blue line is the velocity
 426 model at the SWIR 65-66°E³².



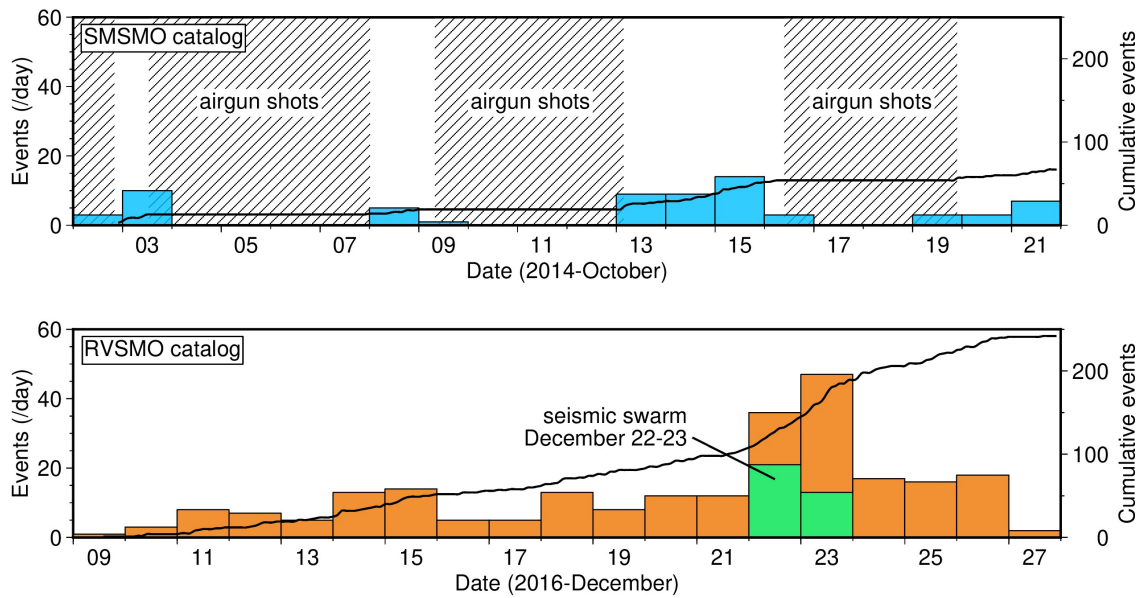
427

428 **Supplementary Fig. 3 | Wadati diagram.** (a) P-wave onset from origin versus S-P time
 429 (Wadati diagram) for both SMSMO (orange) and RVSMO (blue) catalogs. (b) Histogram of
 430 V_p/V_s ratio. V_p/V_s ratio is calculated from the slopes of the Wadati diagram. The best-fitting
 431 V_p/V_s ratio is 1.7.



432

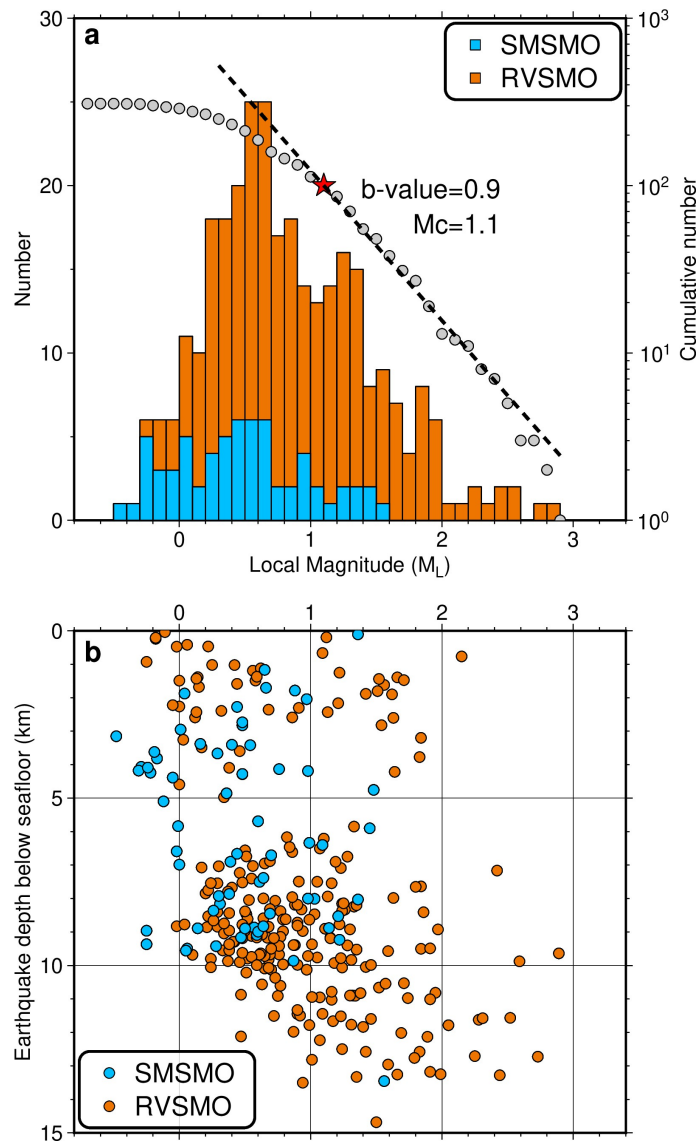
433 **Supplementary Fig. 4 | Station corrections of P- and S-wave returned by NonLinLoc.**



434

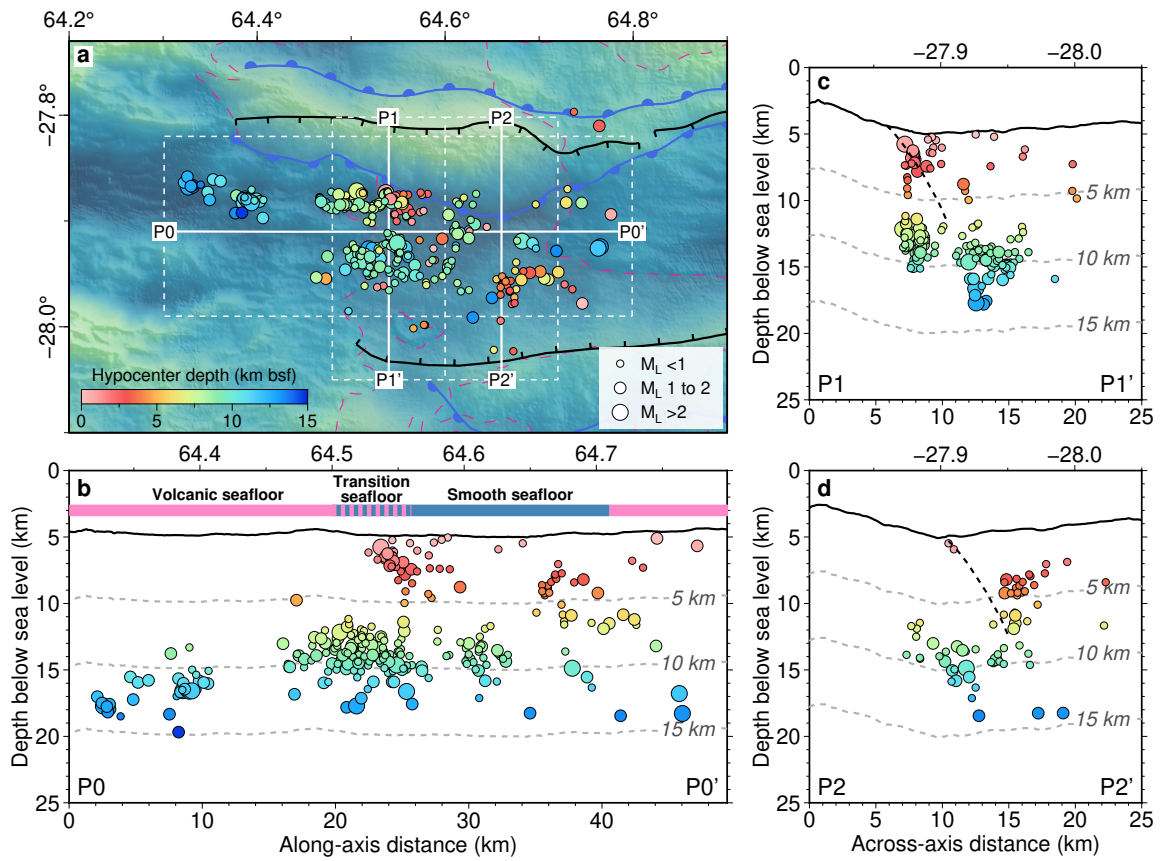
435 **Supplementary Fig. 5 | Histogram and cumulative histogram of located earthquakes for**
 436 **the SMSMO and RVSMO catalogs.**

437



438

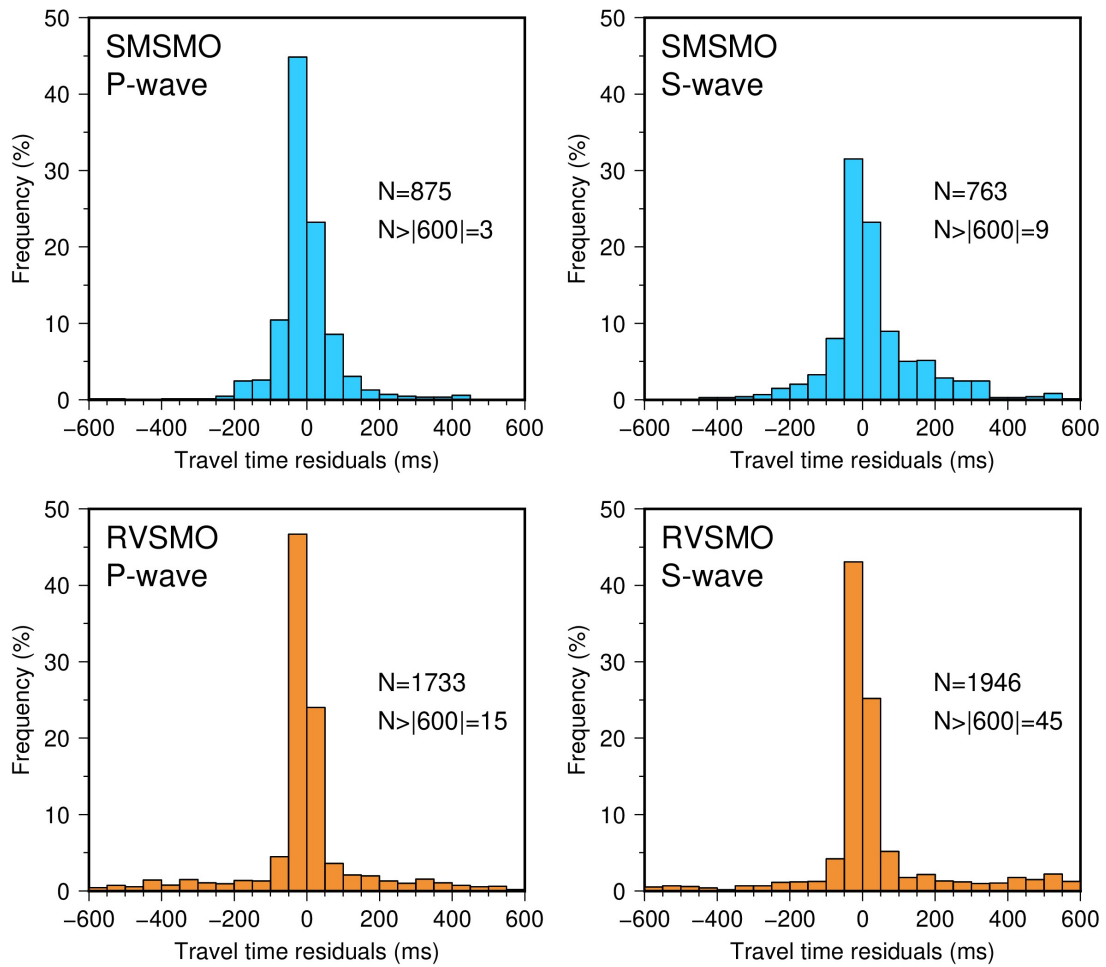
439 **Supplementary Fig. 6 | Distribution of local magnitude (M_L).** (a) Histograms of local
 440 magnitude for the SMSMO (blue) and RVSMO (orange) catalogs (left Y-axis). The
 441 cumulative number of earthquakes for both catalogs (gray circles) as a function of local
 442 magnitude (right Y-axis). Magnitude completeness (M_c) is determined as 1.1 (red star) using
 443 the b-value stability approach⁴⁷, resulting in a b-value of 0.9 (slope of the dashed line). (b)
 444 Local magnitude as a function of earthquake depth for the SMSMO (blue) and RVSMO
 445 (orange) catalogs.



446

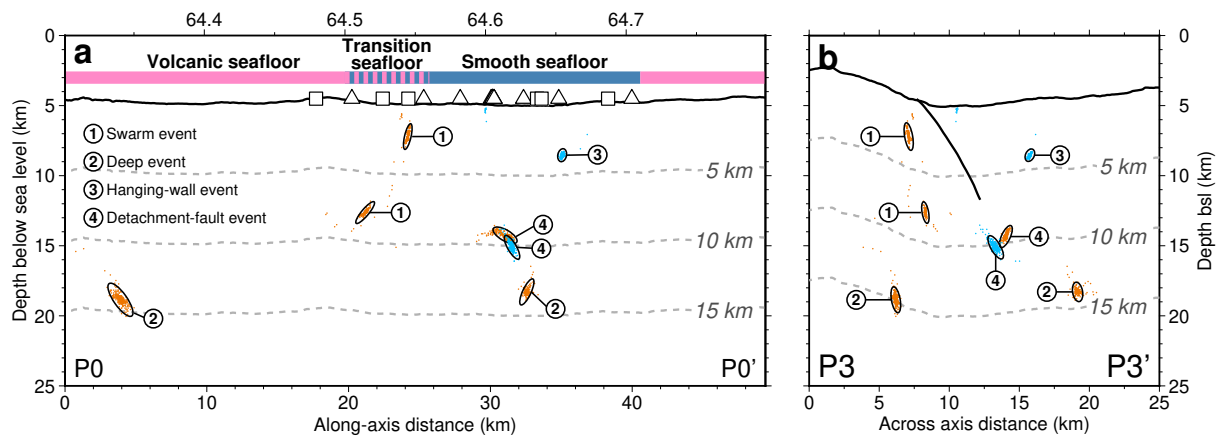
447 **Supplementary Fig. 7 | Earthquake relocations, color coded based on hypocenter depths**
 448 **and circle size based on local magnitude (M_L).**

449



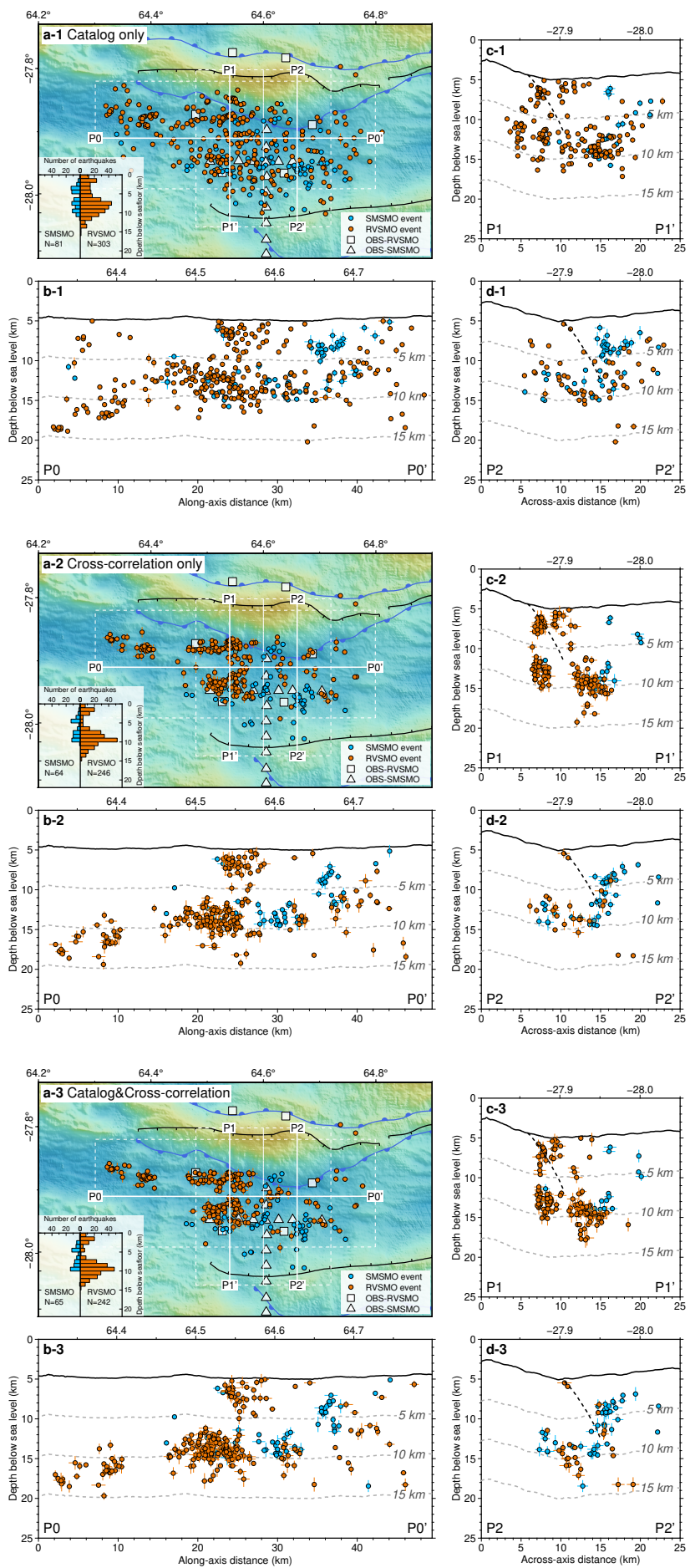
456

457 **Supplementary Fig. 9 | Frequency distribution of P- and S-wave travel time residuals**
 458 **for the SMSMO (blue) and RVSMO (orange) catalogs.**



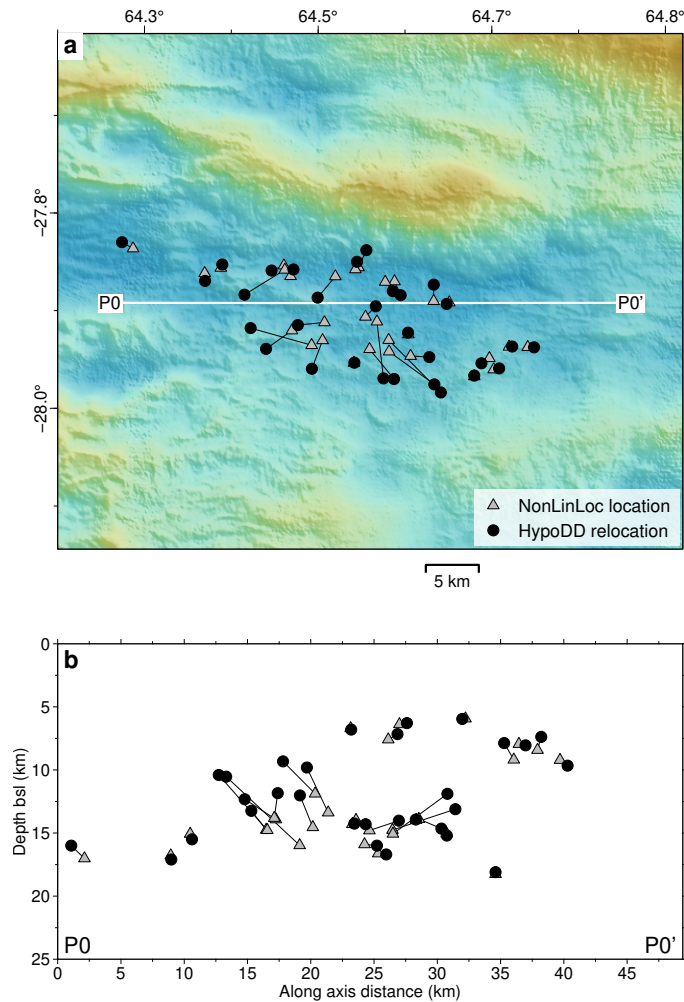
459

460 **Supplementary Fig. 10 | Bootstrap analysis of location errors for four chosen groups of**
 461 **NonLinLoc located events.** Blue and orange dots represent events in the SMSMO and
 462 RVSMO catalogs, respectively. Perturbations were randomly applied 300 times to P and S
 463 arrivals, which were constrained by travel time residuals shown in Supplementary Fig. 9.



465 **Supplementary Fig. 11 | Earthquake relocations.** See legend for symbols. Tests of
466 earthquake relocation using the HypoDD with catalog only (**a-1** to **d-1**), cross-correlation
467 only (**a-2** to **d-2**), and catalog&cross-correlation (**a-3** to **d-3**; same results as Fig. 2). Error
468 bars represent relative location errors.

469



470

471 **Supplementary Fig. 12 | Differences of NonLinLoc locations and HypoDD relocations**
472 **for 30 randomly selected events.** Each event is connected by a black line between the
473 results of the NonLinLoc location and the HypoDD relocation (catalog&cross-correlation).
474 (a) Map view. (b) events projected on the along-axis P0-P0' profile.

475